photonics

IMPACT FACTOR 2.1

CITESCORE 2.6

Article

Expansion Dynamics of Rydberg-Dressed Ultracold Fermi Gas

Meimei Wu, Xin Bao, Shuxian Yu, Shujin Deng and Haibin Wu

MDPI

https://doi.org/10.3390/photonics12040350

photonics

MDPI

Article

Expansion Dynamics of Rydberg-Dressed Ultracold Fermi Gas

Meimei Wu [1], Xin Bao [1], Shuxian Yu [1], Shujin Deng [1,*] and Haibin Wu [1,2]

[1] Institute of Quantum Science and Precision Measurement, East China Normal University, Shanghai 200062, China
[2] Collaborative Innovation Center of Extreme Optics, Shanxi University, Taiyuan 030006, China
* Correspondence: sjdeng@lps.ecnu.edu.cn

Abstract: We present a theoretical investigation into the expansion dynamics of Rydberg-dressed ultracold Fermi gases. The effective interaction potential induced by Rydberg dressing significantly modifies the intrinsic properties and dynamical behavior of the quantum gas. The strength and range of these interactions can be precisely tuned by varying the intensity and detuning of the applied laser field. By employing mean-field theory and utilizing the density distribution of the atomic cloud to describe the quantum system dynamics, we theoretically describe the time-dependent evolution of the atomic cloud during the free expansion process, encompassing both non-interacting and unitary Fermi gases. Notably, the specific quantum states of the ground-state atoms play a pivotal role in shaping the effective interaction potential within the Rydberg-dressed quantum system. We elucidate how the interaction potential influences the rate and mode of the atom cloud's expansion by hydrodynamic expansion arising from Rydberg-dressed atoms in distinct spin hyperfine states. This investigation may deepen our understanding of the behavior and interactions in quantum many-body systems and offer broad potential for future applications like the exploration of novel quantum phase transitions and emergent phenomena.

Keywords: Rydberg-dressed ultracold Fermi gases; mean-field theory; time-dependent evolution

Received: 3 March 2025
Revised: 22 March 2025
Accepted: 3 April 2025
Published: 8 April 2025

Citation: Wu, M.; Bao, X.; Yu, S.; Deng, S.; Wu, H. Expansion Dynamics of Rydberg-Dressed Ultracold Fermi Gas. *Photonics* **2025**, *12*, 350. https://doi.org/10.3390/photonics12040350

1. Introduction

Ultracold atomic gases provide a versatile platform for studying quantum many-body physics. Controlling inter-particle interactions in such quantum systems is of paramount importance for the exploration of novel phases of matter and the investigation of many-body quantum dynamics [1–4]. Recently, efforts have been focused on the study of dipolar physics, where strong non-local interactions ensure the realization of novel many-body phases, like self-organization criticality [5], supersolidity [6], and superradiant quantum phase transitions [7]. The regime of strong dipolar couplings is easily realized by exciting atoms to Rydberg states, which have highly excited valence electrons with a principle quantum number of $n \gg 1$ [8]. Typically, Rydberg atoms decay on a timescale of tens of microseconds, which is very short relative to the overall millisecond timescale of motion. Rydberg dressing effectively addresses this issue by exciting only a small number of atoms to Rydberg states. Rather than a direct excitation to the Rydberg state, Rydberg dressing can be used to obtain both long-lifetime and large dipolar interactions [9,10].

Owing to the highly controllable and tunable long-range interactions inherent to Rydberg atoms, it is possible to simulate quantum systems with a wide range of interaction strengths. This capability also offers a novel and powerful approach to investigating quantum information science and quantum computing [11–13]. Due to the interaction between

Rydberg atoms and background gases, particular shell-shaped structures are formed in the quantum state [14,15]. Additionally, bosons and fermions play significant roles in quantum statistics, causing Rydberg-dressed ultracold bosonic and fermionic atomic gases to exhibit extremely different many-body phenomena [16,17]. Experimental research on Rydberg dressing has predominantly focused on the interaction between Rydberg bosonic atoms [18–20]. For ultracold Fermi gases, due to the Fermi–Dirac exclusion principle, the interaction between atoms can be stably controlled, which provides a powerful tool for manipulating non-local Rydberg long-range interactions. In recent years, many theoretical works have examined Rydberg-dressed Fermi gases [21,22], while more experimental research still needs to be conducted. In experiments, ultracold Fermi gases are typically cooled to near absolute zero using laser cooling techniques with fermions (e.g., ^{6}Li and ^{40}K). At low temperatures, the quantum properties of ultracold Fermi gases begin to dominate, exhibiting Fermi–Dirac statistical behavior, phase transitions, and sensitivity to external interactions. In particular, Rydberg-dressed Fermi gases combine the strong dipolar interaction with the unique quantum statistical behavior of fermionic systems, which provides a new perspective for people to explore the many-body physics related to strongly correlated quantum phenomena and offers possibilities for research on exotic phases [23,24]. Compared with the short-range interactions in traditional ultracold atomic systems, a Rydberg-dressed ultracold Fermi gas can precisely control non-local interactions by adjusting the intensity and range of Rydberg excitation. For Rydberg-dressed atomic fermions in three-dimensional optical lattices, the existence of various topological density waves has been predicted, and their topological properties and phase transition behaviors have been analyzed [24]. This has provided a new platform for the study of topological density waves, which has significant theoretical significance and experimental value. In a recent experiment, ^{6}Li atoms were loaded into a two-dimensional optical lattice, where they were excited to a Rydberg state by a single step with a UV laser. By adjusting the laser intensity to control the non-local interaction in real time, it was experimentally observed that this non-local interaction significantly slowed down the density relaxation dynamics of the gas [25]. This provides new opportunities to explore the many-body phase transitions associated with Rydberg-dressed fermions [21,23,26].

In this article, we studied the expansion dynamics of Rydberg-dressed Fermi gases in a three-dimensional harmonic trap. The expansion dynamics of ultracold Fermi gases is well described by time-dependent hydrodynamics [27,28], showing the well-known anisotropic expansions [29]. Thanks to the scale invariance, the evolution of the cloud can be simply tracked by scaling equations [30–32]. One can use time-dependent scaling factors $\lambda(t) = \sigma(t)/\sigma(0)$ to describe the evolution of the system, where $\sigma(t)$ is the cloud size at different times t. Here, we theoretically extended this method to a Rydberg-dressed Fermi gas. We considered the Rydberg nS states, shown in Figure 1, which exhibit isotropic dipolar interactions. The Rydberg-dressed scheme enables a long lifetime for the observation of hydrodynamics and, thus, could be treated as an increase in the interaction energy without angular dependence. By checking the density distributions, we found that the expansions were clearly anisotropic, even with Rydberg nS states, which is deeply associated with hydrodynamics. By changing the principle number n, a positive correlation between the principal quantum number and anisotropy was identified. Moreover, a slightly broken scale invariance was found during the expansion dynamics. Our results establish the possibility of tailoring the dynamics of Rydberg-dressed quantum gases far from equilibrium.

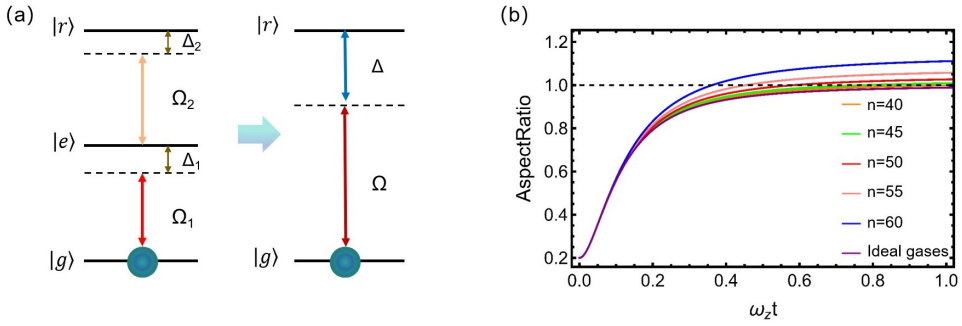

Figure 1. (**a**) Schematic figure of two-photon excitation with Rydberg dressing. By carefully selecting the parameters, the intermediate ($|e\rangle$) states could be adiabatically eliminated from the system. $\Delta_{1,2}$ and $\Omega_{1,2}$ are the detuning and Rabi frequencies corresponding to ($|g\rangle$) to ($|e\rangle$) and ($|e\rangle$) to ($|r\rangle$), respectively. The right panel is an effective figure, where Ω and Δ are the effective Rabi frequency and detuning. (**b**) The evolution of the aspect ratio for a non-interacting Fermi gas in state $|2\rangle$ with different Rydberg dressing schemes. The aspect ratio of the cloud would break the ballistic expansion and gradually exceed 1 at high Rydberg states. A cloud dressed with a higher principle number would show a larger aspect ratio.

2. Method: Mean-Field Hydrodynamical Description

We first consider the Hamiltonian of a balanced two-component Fermi gas with Rydberg dressing [33,34]:

$$\widehat{H} = \int d\mathbf{r}\hat{\Phi}^{\dagger}(\mathbf{r})\left[-\frac{\hbar^2}{2m}\nabla^2 + V_{ext}(\mathbf{r})\right]\hat{\Phi}(r) + \frac{1}{2}\int d\mathbf{r}d\mathbf{r}'\hat{\Phi}^{\dagger}(\mathbf{r})\hat{\Phi}^{\dagger}(\mathbf{r}')V_{mf}(\mathbf{r}-\mathbf{r}')\hat{\Phi}(\mathbf{r}')\hat{\Phi}(\mathbf{r}), \tag{1}$$

where $V_{ext}(\mathbf{r})$ is the external potential, and the mean-field potential $V_{mf}(\mathbf{r}-\mathbf{r}')$ can be divided into two parts:

$$V_{mf}(\mathbf{r},t) = gn(\mathbf{r},t) + \int d\mathbf{r}' U_{Ryd}(\mathbf{r}'-\mathbf{r})n(\mathbf{r}',t), \tag{2}$$

where the first term describes the inter-particle interaction, and the second term is the induced energy with Rydberg excitation. The coupling constant g is related to the scattering length a_s by $g = 4\pi a_s\hbar^2/\mathrm{m}$, where a_s is the strength of the interatomic interactions. By introducing the Euler equations $\frac{\partial}{\partial t}n + \boldsymbol{\nabla}\cdot(\mathbf{v}n) = 0$, we can derive the following equation of the velocity field:

$$m\frac{\partial}{\partial t}\mathbf{v} = -\boldsymbol{\nabla}\cdot\left(-\frac{\hbar^2\nabla^2\sqrt{n}}{2m\sqrt{n}} + \frac{mv^2}{2} + V_{ext} + gn + \int d\mathbf{r}' U_{Ryd}(\mathbf{r}'-\mathbf{r})n(\mathbf{r}',t)\right), \tag{3}$$

Then, we introduce the phase space density of atoms $f(t,r_i,v_i) = f(t,x,y,z,v_x,v_y,v_z)$ to predict the time evolution equation of Rydberg-dressed Fermi gases. The dynamics of gas are described by the total time derivative of the phase space density [35,36]:

$$\frac{\partial f}{\partial t} + \mathbf{v}\cdot\frac{\partial f}{\partial \mathbf{r}} - \frac{1}{m}\frac{\partial(V_{ext}+V_{mf})}{\partial \mathbf{r}}\cdot\frac{\partial f}{\partial \mathbf{v}} = I_{coll}[f], \tag{4}$$

where $I_{coll}[f]$ is an integral associated with the gas collision process. In this paper, we address the collision integral using the relaxation time approximation, $I_{coll}(f) \approx \frac{-(f-f_{le})}{\tau_R}$, where τ_R is the relaxation time related to the average time between collisions, and f_{le} is the local equilibrium density in the phase space.

Through a coordinate transformation, the initial coordinate r_i is converted to a time-dependent coordinate R_i. The phase space density function is rewritten as a scalar equation, $f(t,r_i,v_i) = \frac{1}{\prod_j(\lambda_j\theta_j^{1/2})}f_0(\frac{r_i}{\lambda_i}, \frac{1}{\theta_i^{1/2}}(v_i - \frac{\dot{\lambda}_i}{\lambda_i}r_i))(j = x,y,z)$, where f_0 is the equilibrium distri-

bution function that satisfies the equation $I_{coll}[f_0] = 0$. The scaling parameter $\lambda_i = \lambda_i(t)$ gives the dilation along the ith direction, while $\theta_i = \theta_i(t)$ gives the effective temperature in the same direction. We define the following ansatz for the nonequilibrium distribution function: $f(\mathbf{r}, \mathbf{v}, t) = f_0(\mathbf{R}(t), \mathbf{V}(t))$, with $R_i = \frac{r_i}{\lambda_i}$, $V_i = \lambda_i v_i - \dot{\lambda}_i r_i$. This analysis incorporates the particle density distribution implicitly, while the dependence on time is included in the free parameter λ_i. The dynamics of a non-interaction Fermi gas in a harmonic trap can be expressed as

$$\frac{V_i}{\lambda_i^2}\frac{\partial f_0}{R_i} - \lambda_i R_i(\ddot{\lambda}_i + \omega_i^2\lambda_i)\frac{\partial f_0}{\partial V_i} - \frac{g}{m\prod_j \lambda_j}\frac{\partial n_0}{\partial R_i}\cdot\frac{\partial f_0}{\partial V_i} = 0, \tag{5}$$

Considering an ultracold Fermi gas confined in a harmonic trap, the virial theorem can be expressed as $2E_{kin} - 2E_{ho} + 3E_{int} = 0$, where E_{kin}, E_{ho}, and E_{int} are the kinetic energy, harmonic potential, and interaction energy, respectively [27]. The applicability of the virial theorem can help us understand how to control the quantum system's properties by controlling the interaction potentials. For simplicity, we can transform Equation (5) into

$$\ddot{\lambda}_i + w_i^2\lambda_i - \frac{w_i^2}{\lambda_i^3} + \frac{3}{2}w_i^2\frac{E_{int}}{E_{ho}}\left(\frac{1}{\lambda_i^3} - \frac{1}{\lambda_i\prod_j \lambda_j}\right) = 0, (i = x,\ y,\ z), \tag{6}$$

where we can see that the expansion dynamics can be simply described by the interaction energy. Equation (6) would fall back to ballistic expansion while the interaction energy E_{int} is zero, which means that the cloud would eventually evolve into a sphere for a long expansion time. A detailed theoretical description of the energy of this part of the quantum system is provided in Appendix A.

3. Results and Discussion

Here, we consider the ^{6}Li Fermi gas confined in a cigar-shaped harmonic trap. A schematic configuration of the Rydberg dressing can be seen in Figure 1a, where a two-photon Rydberg excitation process with off-resonant coupling dresses the atoms to Rydberg nS states. The $|g\rangle$ state is considered to be one of the lowest hyperfine states, $|1\rangle = |F = 1/2, M_F = +1/2\rangle$ or $|2\rangle = |F = 1/2, M_F = -1/2\rangle$. The ground-state $|g\rangle = |2S_{1/2}\rangle$ is coupled to state $|2P_{3/2}\rangle$ and then to $|r\rangle = |nS_{1/2}\rangle$ via σ^- and σ^+ transitions. The Rabi frequency and the detuning of the first photon transition are Ω_1 and Δ_1, respectively. For the second photon transition, we have the Rabi frequency Ω_2 and the detuning Δ_2. For $|\Delta_1| \gg |\Omega_1|$, the intermediate state can be adiabatically eliminated. This results in an effective two-level system with $|g\rangle$ and $|r\rangle$, which have effective Rabi frequencies and detunings, $\Omega = \Omega_1\Omega_2/2\Delta_1$ and $\Delta = \Delta_1 + \Delta_2$, respectively. The parameters taken in this study are as follows: the trap frequencies are $\omega_x = \omega_y = 2\pi \times 200$ Hz and $\omega_z = 2\pi \times 40$ Hz, the effective Rabi frequency is fixed to 3 MHz, and the effective detuning of the two-photon process is fixed to 80 MHz with respect to state $|2\rangle$. This leads to a weaker coupling to the atoms in state $|1\rangle$ due to the larger detuning and thus exhibits spin-dependent dynamics. For this experimental situation, the lifetime of Rydberg states with a principle number n larger than 40 would be more than 100 ms, about one to two orders larger than the typical time scale of the trap. Here, we neglected the dissipations during the expansion.

We begin by studying the dynamical expansion of a Rydberg-dressed non-interacting Fermi gas, where the two lowest hyperfine states $|1\rangle$ and $|2\rangle$ do not collide with each other. This is quite a simple situation, and the excitation laser dresses the atoms with different detunings. A Feshbach resonance is used to tune the interaction of the atoms either to the non-interacting regime with a magnetic field of B = 528 G or to the unitary limit with

B = 832 G. For the non-interacting case, the hyperfine splitting between the two hyperfine states is 75.6 MHz, while the value is 76.3 MHz for the unitary limit.

We study the expansion dynamics by numerically solving the dynamic Equation (6) for Rydberg-dressed atoms with different quantum numbers ($n = 40 \rightarrow 60$), taking the initial boundary conditions for the atoms as $\lambda_i = 1$, $\dot{\lambda}_i = 0$. The results can be seen in Figure 1b, where the atoms are released from the anisotropic harmonic trap, with the initial aspect ratio set to 0.2. We change the interaction by exciting the cloud to different Rydberg states with the same detuning and Rabi frequency. The aspect ratio of the cloud is defined as $\sigma_x(t)/\sigma_z(t) = (\omega_z\lambda_x(t))/(\omega_x\lambda_z(t))$ by taking the initial condition as a thermal equilibrium state.

In Figure 1b, we can see that the aspect ratio of the cloud in state $|2\rangle$ eventually approaches 1 without Rydberg dressing, showing a typical ballistic expansion process. Otherwise, as the Rydberg state increases, the asymptotic value of the aspect ratio after evolution gradually exceeds 1, which could be regarded as hydrodynamical evolution [29]. When the principle number of the Rydberg states increases, the larger dipole interaction certainly makes the system strongly interacting and leads to a higher aspect ratio.

We observe spin-dependent expansion dynamics for the Rydberg-dressed non-interacting Fermi gas. As hyperfine splitting can be compared with the effective detuning of Rydberg excitation, two-photon excitation would induce a spin-dependent interaction strength, leading to spin-dependent expansion dynamics, as shown in Figure 2a. The expansion dynamics of the atoms in state $|1\rangle$ approach the ballistic expansion, indicating quite a weak interaction strength. Nonetheless, the aspect ratio of the atoms in state $|2\rangle$ shows quite different behavior, which is shown in Figure 2b. The Rydberg-dressed interaction mainly reduces the expansion rate in the axial direction, making the ensembles anisotropic for a long time of flight (TOF), which is similar to the expansion dynamics in strongly interacting Fermi gases [29,37].

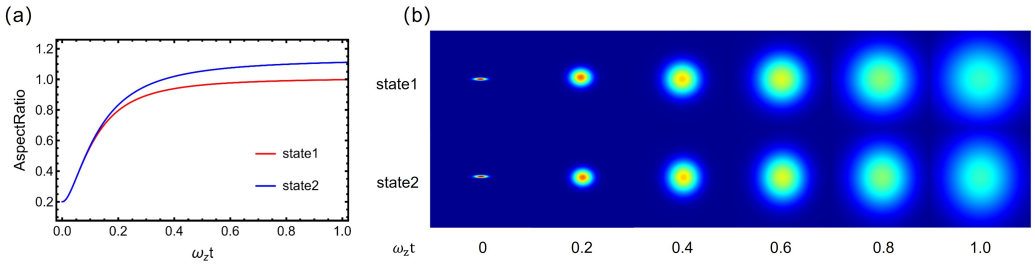

Figure 2. (**a**) The dynamical evolution of aspect ratios for different hyperfine states $|1\rangle$ and $|2\rangle$ when dressed with $n = 60$ Rydberg states. (**b**) The density distribution of states $|1\rangle$ and $|2\rangle$ with different times of flight (TOFs) in the unit of $\omega_z t$. The atoms are partially excited to $n = 60$ Rydberg states, with the Rabi frequency set to 3 MHz and an 80 MHz detuning from the $|2\rangle$ state.

Furthermore, we extend our study to the unitary regime. The strong scattering between atoms redistributes the energy and momentum simultaneously, leading to the strong coupling of the expansion dynamics for different spins. The expansion dynamics at unitarity may thus be rewritten in the following formula:

$$\ddot{\lambda}_i + \omega_i^2\lambda_i - \frac{\omega_i^2}{\lambda_i\prod_j\lambda_j^{2/3}} + \frac{3}{2}\omega_i^2\frac{E_{int}}{E_{ho}}\left(\frac{1}{\lambda_i\prod_j\lambda_j^{2/3}} - \frac{1}{\lambda_i\prod_j\lambda_j}\right) = 0,\ (i = x, y, z), \quad (7)$$

However, quite a small deviation is found for the unitary Fermi gas with or without Rydberg dressing, where both scenarios show obvious anisotropic expansion. This means that the scattering interaction between two hyperfine states is sufficiently large and dominates the expansion dynamics. Nonetheless, the Rydberg interaction would eventually increase the

aspect ratio at sufficiently long TOFs due to the enhancement of the interaction, which can be seen in Figure 3.

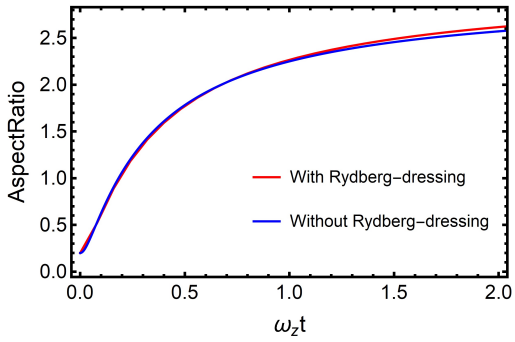

Figure 3. The evolution of the aspect ratio for unitary Fermi gases with Rydberg dressing (red line) and without Rydberg dressing (blue line), where the principal quantum number n of Rydberg atoms is set to 60, with all other parameters unchanged.

To further analyze the anisotropic expansion dynamics of a Fermi gas with Rydberg dressing, we test the scale invariance by tracking the mean square cloud size $\langle r^2 \rangle = \langle x^2 + y^2 + z^2 \rangle$. The scale invariance of the expanding gas can be determined by measuring $\tau^2(t) \equiv m[\langle r^2 \rangle - \langle r^2 \rangle_0]/\langle x \cdot \bigtriangledown U_{opt} \rangle_0$. For a scale-invariant system, the values of $\tau^2(t)$ are independent of the initial density distribution and obey the formula $\tau^2(t) = t^2$, which has already been demonstrated in Refs. [28,38].

However, the breaking of scale invariance symmetry was found in the Rydberg-dressed Fermi gas, as shown in Figure 4. The emergence of a new length scale due to the Rydberg dressing breaks the symmetry by slowing down the overall expansion dynamics. After fitting the data for the Rydberg-dressed Fermi gas, we found $\chi^2 t^2$ scalings for both the non-interacting and unitary Fermi gases. The expansion dynamics fell on the same curve, with χ^2 being about 0.91, which means that non-local Rydberg interactions break the symmetry at a longer spatial scale with hardly any connections to the short-range scattering interaction. This potentially offers a new method for manipulating many-body dynamics with a high controllable interaction strength and diverse spatial dimensions.

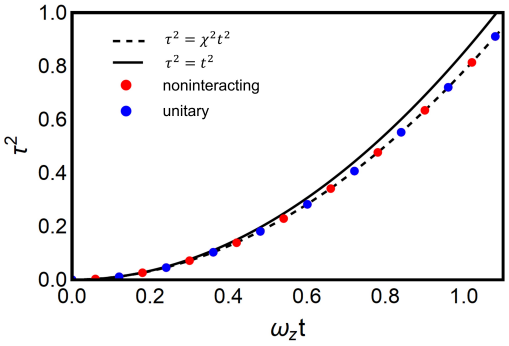

Figure 4. Scale-invariant expansion of a Rydberg-dressed Fermi gas. The blue and red dots represent the non-interacting and unitary Fermi gases with Rydberg dressing, while the black solid line represents scale-invariant expansion. The black dashed line is best fit with $\tau^2 = \chi^2 t^2$, where χ^2 is 0.91.

4. Conclusions

In conclusion, we found that the long-range interactions induced by Rydberg dressing continued to influence particle interactions during the free expansion of the atomic ensemble. The effective interaction potential induced by Rydberg dressing significantly modified the intrinsic properties and dynamical behavior of the quantum gas. Although the

atomic gas was dressed with isotropic nS Rydberg states, these interactions generated an anisotropic expansion during the TOF of a non-interacting Fermi gas with Rydberg dressing. Additionally, we observed spin-dependent anisotropic expansion, which could be used to manipulate different states with long-range interactions. In the unitary regime, where the scattering length diverged, the expansion times with the Rydberg-dressed interaction barely changed the evolution of the aspect ratio. By checking the scale invariance during the TOF, we found clear symmetry breaking for both non-interacting and unitary Fermi gases with Rydberg dressing.

Compared with the short-range interactions in ultracold Fermi atom systems, the use of Rydberg dressing technology allows for ground-state atoms to be excited into a superposition state composed of the ground state and a highly excited Rydberg state, exhibiting strong long-range interactions. Experimentally, by adjusting the optical field, the non-local long-range interactions between Fermi atoms can be precisely controlled, thereby influencing the nonequilibrium dynamical behavior of the atomic gas. Our results provide predictions for the evolution of the density in different hyperfine states and enable theoretical investigations of the strength and form of dressed interactions, which may offer a new experimental method for testing the hydrodynamics of Rydberg-dressed quantum gases and benefit the understanding of long-range interactions in quantum many-body systems. This would enable the exploration of strongly correlated quantum phenomena in regimes that are otherwise challenging to access.

Author Contributions: Conceptualization, S.D. and H.W.; Investigation, M.W., X.B. and S.Y.; Writing—original draft, M.W. and S.D.; Writing—review & editing, M.W. and S.D.; Supervision, S.D. and H.W.; Project administration, H.W.; Funding acquisition, S.D. and H.W. All authors have read and agreed to the published version of the manuscript.

Funding: This research was supported by the National Key R&D Program of China (2022YFA1404202), Innovation Program for Quantum Science and Technology (2021ZD0302100), National Natural Science Foundation of China (12174105, 11925401, 12234008), Shanghai Rising-Star Program(23QA1402700).

Institutional Review Board Statement: Not applicable.

Informed Consent Statement: Not applicable.

Data Availability Statement: Data are contained within the article.

Conflicts of Interest: The authors declare no conflicts of interest.

Appendix A. Description of Energy in Quantum Systems

To study the energy expression of the Rydberg-dressed Fermi quantum system, the Gross–Pitaevskii (GP) equation can also be derived using a variational procedure $i\hbar\frac{\partial}{\partial t}\Phi = \frac{\delta E}{\delta \Phi^*}$ [39], where the energy functional E is given by

$$E[\Phi] = \int d\mathbf{r}[\frac{\hbar^2}{2m}|\nabla\Phi|^2 + V_{ext}(\mathbf{r})|\Phi|^2 + \frac{g}{2}|\Phi|^4], \tag{A1}$$

The first term on the right side of Equation (A1) is the kinetic energy of the quantum system E_{kin}, the second part is the harmonic energy E_{ho}, and the last one is the mean-field interaction energy E_{int}. Note that the mean-field term E_{int} corresponds to the first correction in the virial expansion for the energy of the gas. The quantum system wave function can be written as $\Phi(\mathbf{r}, t) = \phi(\mathbf{r})exp(-iut/\hbar)$, where u is the chemical potential, and ϕ is real and normalized to the total number of particles, $\int \phi^2 d\mathbf{r} = N$. Then, the GP equation becomes

$$(-\frac{\hbar^2\nabla^2}{2m} + V_{ext}(\mathbf{r}) + V_{mf}(\mathbf{r}))\phi(\mathbf{r}) = u\phi(\mathbf{r}), \tag{A2}$$

The equation takes the form of a 'nonlinear Schrödinger equation', with the nonlinearity arising from the mean-field term, which is proportional to the particle density $n(\mathbf{r}) = \phi^2(\mathbf{r})$. By taking advantage of the tunability of Rydberg-dressed interactions, the interaction potential between the ground-state atoms is significantly enhanced by adjusting the Rabi frequency and detuning the laser field, allowing for the precise control of the dressed interactions over a wider range of parameters.

Rydberg dressing enables the Fermi gas to form both short-range and long-range interactions, thereby modifying the effective interaction potential of the quantum system. In this case, the density distribution depends not only on the external potential field and the properties of the Fermi gas but also on the dressed effects of the Rydberg-state electrons. According to the mean-field Thomas–Fermi (TF) approximation, the density distribution is given by $n(\mathbf{r}) = \frac{4}{3\pi^2}(\frac{m}{\hbar^2})^{3/2}(u - V_{ho}(\mathbf{r}))^{3/2}$. The Rydberg-dressed effect introduces a new long-range interaction potential to the density distribution of a non-interacting Fermi gas, thereby modifying the shape of its central region. In the edge region, the density distribution decreases and approaches zero as r reaches the TF radius $R_{TF} = \sqrt{2}a_{ho}^2\sqrt{\frac{mu}{\hbar^2}}$. The mean-field interaction potential energy term for this quantum system is $E_{int} = \int \frac{1}{2}gn(\mathbf{r})^2 d^3\mathbf{r}$, and the harmonic potential energy term is $E_{ho} = \int V_{ho}(\mathbf{r})n(\mathbf{r})d^3\mathbf{r}$. As the electron wave function of the nS Rydberg state is isotropic, the electron cloud exhibits spherical symmetry. The crucial parameters are $E_{int}/E_{ho} = 1.140681\frac{N^{1/6}a_{Ryd}}{a_{ho}}$, where $a_{Ryd} = \frac{m\pi^2}{24}\frac{\Omega^4}{\hbar|\Delta|^3}R_C^3$ and $a_{ho} = (\hbar/m\omega_{ho})^{1/2}$. By systematically adjusting variables such as the interaction strength, harmonic trap frequency, and particle density, we can optimize the expansion dynamics model to simulate the role of long-range interactions in atomic gases, revealing the impact of Rydberg dressing on the behavior of atomic gases.

References

1. Gross, C.; Bloch, I. Quantum simulations with ultracold atoms in optical lattices. *Science* **2017**, *357*, 995. [CrossRef]
2. Eigen, C.; Glidden, J.A.P.; Lopes, R.; Cornell, E.A.; Smith, R.P.; Hadzibabic, Z. Universal prethermal dynamics of Bose gases quenched to unitarity. *Nature* **2018**, *563*, 221. [CrossRef]
3. Logan, W. C.; Anita, G.; Lei, F.; Cheng, C. Collective emission of matter-wave jets from driven Bose–Einstein condensates. *Nature* **2017**, *551*, 356.
4. Arunkumar, N.; Jagannathan, A.; Thomas, J.E. Designer Spatial Control of Interactions in Ultracold Gases. *Phys. Rev. Lett.* **2019**, *122*, 040405.
5. Helmrich, S.; Arias, A.; Lochead, G.; Wintermantel, T. M.; Buchhold, M.; Diehl, S.; Whitlock, S. Signatures of self-organized criticality in an ultracold atomic gas. *Nature* **2020**, *577*, 481.
6. Norcia, M.A.; Politi, C.; Klaus, L.; Poli, E.; Sohmen, M.; Mark, M.J.; Bisset, R.N.; Santos, L.; Ferlaino, F. Two-dimensional supersolidity in a dipolar quantum gas. *Nature* **2021**, *596*, 357.
7. Zhang, X.; Chen, Y.; Wu, Z.; Juan, Wang, J.; Fan, J.; Deng, S.; Wu, H. Observation of a superradiant quantum phase transition in an intracavity degenerate Fermi gas. *Science* **2021**, *373*, 1359. [CrossRef]
8. Saffman, M.; Walker, T.G.; Molmer, K. Quantum information with Rydberg atoms. *Rev. Mod. Phys.* **2010**, *82*, 2313.
9. Bouchoule, I.; Mϕlmer, K. Spin squeezing of atoms by the dipole interaction in virtually excited Rydberg states. *Phys. Rev. A* **2002**, *65*, 041803.
10. Henkel, N.; Nath, R.; Pohl, T. Three-Dimensional Roton Excitations and Supersolid Formation in Rydberg-Excited Bose-Einstein Condensates. *Phys. Rev. Lett.* **2010**, *104*, 95302.
11. Madjarov, I.S.; Covey, J.P.; Shaw, A.L.; Choi, J.; Kale, A.; Cooper, A.; Pichler, H.; Schkolnik, V.; Williams, J.R.; Endres, M. High-fidelity entanglement and detection of alkaline-earth Rydberg atoms. *Nat. Phys.* **2020**, *16*, 857–861.
12. Evered, S.J.; Bluvstein, D.; Kalinowski, M.; Ebadi, S.; Manovitz, T.; Zhou, H.; Li, S.H.; Geim, A.A.; Wang, T.T.; Maskara, N.; et al. High-fidelity parallel entangling gates on a neutral-atom quantum computer. *Nature* **2023**, *622*, 268–272.
13. Zhang, Z.H.; Zhang, Z.Y.; Han, S.X.; Zhang, Y.Q.; Zhang, G.Q.; Wu, J.Z.; Sovkov, V.B.; Liu, W.L.; Li, Y.Q.; Zhang, L.J.; et al. Microwave-coupled optical bistability in driven and interacting Rydberg gases. *Npj Quantum Inf.* **2025**, *11*, 44.
14. Liebish, T.C.; Schlagmuller, M.; Engel, F.; Nguyen, H.; Balewski, J.; Lochead, G.; Bottcher, F.; Westphal, K.M.; Kleinbach, K.S.; Schmid, T.; et al. Controlling Rydberg atom excitations in dense background gases. *J. Phys. B* **2016**, *49*, 182001.

15. Sous, J.; Sadeghpour, H.R.; Killian, T.C.; Demler, E.; Schmidt, R. Rydberg impurity in a fermi gas: Quantum statistics and rotational blockade. *Rhys. Rev. Res.* **2020**, *2*, 023021.
16. Balewski, J.B.; Krupp, A.T.; Gaj, A.; Hofferberth, S.; Low, R.; Pfau, T. Rydberg dressing: Understanding of collective many-body effects and implications for experiments. *New J. Phys.* **2014**, *16*, 063012. [CrossRef]
17. Gaul, C.; DeSalvo, B.J.; Aman, J.A.; Dunning, F.B.; Killian, T.C.; Pohl, T. Resonant rydberg dressing of alkaline-earth atoms via electromagnetically induced transparency. *Phys. Rev. Lett.* **2016**, *116*, 243001. [CrossRef]
18. Viteau, M.; Bason, M.; Radogostowicz, J.; Maloss, N.; Morsch, O.; Ciampini, D.; Arimondo, E. Rydberg excitation of a bose-einstein condensate. *Laser Phys.* **2013**, *23*, 015502.
19. Schau, P.; Zeiher, J.; Fukuhara, T.; Hild, S.; Cheneau, M.; Macri, T.; Pohl, T.; Bloch, I.; Gross, C. Crystallization in ising quantum magnets. *Science* **2015**, *347*, 14551.
20. Borish, V.; Markovic, O.; Hines, J.A.; Rajagopal, S.V.; Schleier-Smith, M. Transverse-field ising dynamics in a Rydberg -dressed atomic gas. *Phys. Rev. Lett.* **2020**, *124*, 063601.
21. Xiong, B.; Jen, H.H.; Wang, D.W. Topological superfluid by blockade effects in a Rydberg-dressed fermi gas. *Phys. Rev. A* **2014**, *90*, 013631. [CrossRef]
22. Khasseh, R.; Abedinpour, S.H.; Tanatar, B. Phase diagram and dynamics of Rydberg-dressed fermions in two dimensions. *Phys. Rev. A* **2017**, *96*, 053611. [CrossRef]
23. Li, W.H.; Hsieh, T.C.; Mou, C.Y.; Wang D.W. Emergence of a metallic quantum solid phase in Rydberg-dressed fermi gas. *Phys. Rev. Lett.* **2016**, *117*, 035301. [CrossRef]
24. Li, X.; Sarma, S.D. Exotic topological density waves in cold atomic Rydberg-dressed fermions. *Nat. Commun.* **2015**, *6*, 7137. [CrossRef]
25. Guardado-Sanchez, E.; Spar, B.M.; Schauss, P.; Belyansky, R.; Young, J.T.; Bienias, P.; Gorshkov, A.V.; Iadecola, T.; Bakr, W.S. Quench Dynamics of a Fermi Gas with Strong Nonlocal Interactions. *Phys. Rev. X* **2021**, *11*, 021036. [CrossRef]
26. Takei, N.; Sommer, C.; Genes, C.; Pupillo, G.; Goto, H.; Koyasu, K.; Chiba, H.; Weidemüller, M.; Ohmori, K. Direct observation of ultrafast many-body electron dynamics in an ultracold Rydberg gas. *Nat. Commun.* **2016**, *7*, 13449. [CrossRef]
27. Thomas, J.E.; Kinast, J.; Turlapov, A. Damping of a Unitary Fermi Gas. *Phys. Rev. Lett.* **2005**, *95*, 120402. [CrossRef]
28. Elliott, E.; Joseph, J.A.; Thomas, J.E. Observation of Conformal Symmetry Breaking and Scale Invariance in Expanding Fermi Gases. *Phys. Rev. Lett.* **2014**, *112*, 040405. [CrossRef]
29. O'Hara, K.M.; Hemmer, S.L.; Gehm, M.E.; Granade, S.R.; Thomas, J.E. Observation of a Strongly Interacting Degenerate Fermi Gas of Atoms. *Science* **2002**, *198*, 2179. [CrossRef]
30. Moroz S. Scale-invariant Fermi gas in a time-dependent harmonic potential. *Phys. Rev. A* **2012**, *86*, 011601. [CrossRef]
31. Deng, S.; Chenu, A.; Diao, P.; Li, F.; Yu, S.; Coulamy, I.; Campo, A.D.; Wu, H. Superadiabatic quantum friction suppression in finite-time thermodynamics. *Sci. Adv.* **2018**, *4*, 4. [CrossRef]
32. Deng, S.; Diao, P.; Yu, Q.; Campo, A.D.; Wu, H. Shortcuts to adiabaticity in the strongly coupled regime: Nonadiabatic control of a unitary Fermi gas. *Phys. Rev. A* **2018**, *97*, 013628. [CrossRef]
33. Stringari, S. Collective Excitations of a Trapped Bose-Condensed Gas. *Phys. Rev. Lett.* **1996**, *77*, 2360. [CrossRef]
34. Wei, H.; Xiao-Fei, Z.; Deng-Shan, W.; Hai-Feng, J.; Wei, Z.; Shou-Gang, Z. Chiral Supersolid in Spin-Orbit-Coupled Bose Gases with Soft-Core Long-Range Interactions. *Phys. Rev. Lett.* **2018**, *121*, 030404.
35. Pedri, P.; Guéry-Odelin, D.; Stringari, S. Dynamics of a classical gas including dissipative and mean-field effects. *Phys. Rev. A* **2003**, *68*, 043608. [CrossRef]
36. Guéry-Odelin, D. Mean-field effects in a trapped gas. *Phys. Rev. A* **2002**, *66*, 033613.
37. Trenkwalder, A.; Kohstall, C.; Zaccanti, M.; Naik, D.; Sidorov, A.I.; Schreck, F.; Grimm, R. Hydrodynamic Expansion of a Strongly Interacting Fermi-Fermi Mixture. *Phys. Rev. Lett.* **2011**, *106*, 115304. [CrossRef]
38. Wang, L.; Yan, X.; Min, J.; Sun, D.; Xie, X.; Peng, S.; Zhan, M.; Jiang, K. Scale Invariance of a Spherical Unitary Fermi Gas. *Phys. Rev. Lett.* **2024**, *132*, 243403. [CrossRef]
39. Dalfovo, F.; Giorgini, S.; Pitaevskii, L.P.; Stringari, S. Theory of Bose-Einstein condensation in trapped gases. *Rev. Mod. Phys.* **1999**, *71*, 463. [CrossRef]